

Big Fiber Slicing for Dynamic Multimodal Multipreference Applications of Smart Fabrics

Jia Liu¹, Huanke Zheng, Dongkun Huo, *Member, IEEE*, Yixue Hao, Dusit Niyato², *Fellow, IEEE*, Salman A. Alqahtani³, and Min Chen⁴, *Fellow, IEEE*

Abstract—In recent years, significant breakthroughs have been achieved in smart fabric technology within the healthcare sector, providing an impetus for the smart integration of wearable devices and equipment in medical applications. However, the tight coupling between fabric hardware devices and software solutions, tailored for various scenarios, has led to inefficient utilization of hardware resources and led to challenges for device upgrades and iterations. This article focuses on the virtualization technology of smart fabric hardware resources and introduces a novel approach, termed “Big Fiber Slicing.” First, we outline the design of novel fiber devices customized for two major application scenarios: health monitoring and protection. Subsequently, we delve into the process of partitioning hardware resources into multiple “fiber slices” to better meet the unique requirements of various application scenarios and services. Next, we built a smart fabric platform, combined with 5 real multimodal applications with different preferences, to verify the performance of the system when resources are limited and demand changes dynamically. Lastly, we explore the potential challenges that smart fabric technology may encounter in future application scenarios and provide insights into the future direction of this field.

Index Terms—Healthcare, MAPPO, sensor virtualization, smart fabrics.

I. INTRODUCTION

NETWORK slicing, as a cornerstone of 5G networks, has demonstrated its efficacy through widespread applications. It allows network operators to offer tailored network services for diverse scenarios. By creating multiple independent virtual networks (known as “slices”) within a single physical network, each slice can be finely tuned to meet

the specific requirements of an application. This approach ensures efficient resource utilization, flexible service delivery, and superior user experiences [1] [2]. This innovation idea paves the way for handling a wider array of tasks, especially in situations that necessitate the elastic allocation of hardware resources in response to application-specific requirements.

Meanwhile, over the past few years, the development of multimaterial functional fiber manufacturing technologies [3] has emerged, capturing global attention. Particularly, the advent of smart fabrics and wearable technology has ushered in a transformative era in healthcare. Through the integration of digital technology into the daily used fabric, e.g., clothes people wear, sofa, and carpet, etc., smart systems empowered by big fiber now have the capabilities to monitor [4], diagnose [5], and even treat health conditions [6] in the ways that were previously infeasible. However, a challenging issue exists in the design of smart fabric systems, i.e., the hardware resources of functional fibers should be software-defined to extend their functionalities for various application scenarios.

When big fiber meets 5G slicing technique, this article proposes the concept of “Big Fiber Slicing.” By the introduction of network slicing technique, big fiber slicing aims to decouple fabric hardware and software, ensuring that users’ evolving and varied application requirements are met in environments with multimodal and heterogeneous fiber devices.

At its core, the “Big Fiber Slicing” method involves segmenting the hardware resources of smart fabrics into multiple independent “slices,” as shown in Fig. 1. Specifically, we virtualize physical sensors according to different processing methods of sampling, preprocessing, and data compression. Our reinforcement learning algorithm is then employed to allocate nodes in the virtual sensor pool, tailoring to the application’s diverse requirements within the constraints of computing power and network bandwidth. This optimization leads to enhanced overall resource utilization, simplified upgrades and iterations, and improved adaptability and scalability of the devices.

The contributions of this article are as follows.

- 1) We propose a method for virtualizing hardware resources in smart fabrics, which we refer to as the “Big Fiber Slicing” approach. This method is designed to address the dynamic and multimodal multipreference application requirements within the system.
- 2) We have established a real fabric platform and validated the performance of our proposed solution under conditions of resource constraints and dynamic changes in

Manuscript received 22 January 2024; revised 11 March 2024; accepted 14 March 2024. Date of publication 29 March 2024; date of current version 7 June 2024. This work was supported by the Distinguished Scientist Fellowship Program, King Saud University, Riyadh, Saudi Arabia, under Grant DSFP2024. (Corresponding authors: Yixue Hao; Min Chen.)

Jia Liu, Dongkun Huo, and Yixue Hao are with the School of Computer Science and Technology, Huazhong University of Science and Technology, Wuhan 430074, China (e-mail: jialiu0330@hust.edu.cn; dongkunhuo@hust.edu.cn; yixuehao@hust.edu.cn).

Huanke Zheng is with the School of Computer Science and Engineering, South China University of Technology, Guangzhou 510640, China (e-mail: 202320143150@mail.scut.edu.cn).

Dusit Niyato is with the School of Computer Engineering, Nanyang Technological University, Singapore (e-mail: dniyato@ntu.edu.sg).

Salman A. Alqahtani is with the Department of Computer Engineering College of Computer and Information Sciences, King Saud University, Riyadh 11451, Saudi Arabia (e-mail: salmanq@ksu.edu.sa).

Min Chen is with the School of Computer Science and Engineering, South China University of Technology, Guangzhou 510640, China, and also with the PZhou Laboratory, Guangzhou 510640, China (e-mail: minchen@ieee.org).

Digital Object Identifier 10.1109/JIOT.2024.3380640

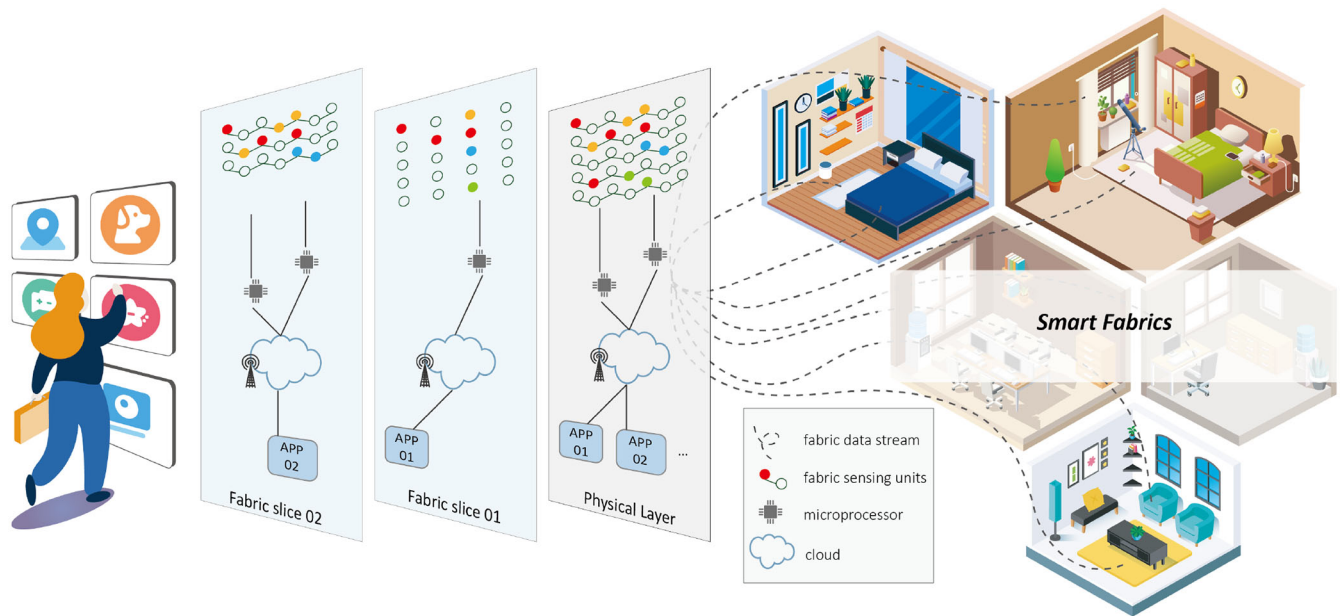


Fig. 1. Concept of big fiber slicing in fabric smart spaces.

application demands, driven by real-world application requirements.

The remainder of this article is organized as mentioned below. In Section II, we present a retrospective of recent developments in the field of fiber-based novel materials and devices designed for health monitoring and prevention. Section III describes the architecture of hardware resource virtualization and slicing techniques within the smart fabric space. The discussion in Sections IV and V will delve into the analysis models and the FS-MAPPO algorithm. In Section VI, we built a real smart fabric testbed and conducted experiments. Section VII addresses the challenges that smart fabric technologies face when dealing with health-related issues in medicine. Finally, Section VIII concludes this article, and we provide an outlook for future research directions.

II. OVERVIEW OF FIBER DEVICES FOR HEALTHCARE AND RELATED WORK

With advancements in manufacturing techniques, smart fabrics have been developed to possess remarkable sensing capabilities [7]. These fibers can sense forces, heat, humidity, and various environmental and physiological factors, making them revolutionary for ubiquitous health monitoring technologies. Beyond these crucial functions, smart fibers can also seamlessly integrate into daily life without disrupting the user's routine. In this section, we summarize the applications of smart fibers used for monitoring physiological, motion and thermal/humidity parameters.

The human body emits a multitude of physiological signals that serve as reflections of an individual's health. These signals can provide pivotal early warnings and assessments for sudden illnesses. Compared to conventional medical monitoring devices, smart fabrics offer distinct advantages, primarily their portability and real-time data capabilities. Their applications

are broad, and they rely on different sensing principles such as piezoelectricity [8], triboelectricity [9], and optics [10], which enable monitoring variables like electrocardiograms, respiration, and pulse.

A notable example in the field is the work of Li et al. [11], who developed PVDF/DA nanofibers with significantly enhanced piezoelectric performance. These fibers exhibit excellent stability and biocompatibility, and they respond with high sensitivity and accuracy to physiological mechanical stimuli, such as diaphragm movement and blood pulsation. The potential of these fibers was evident when tested on human skin and inside mouse bodies.

Another significant milestone is the work by Wang et al. [9], who demonstrated the applicability of triboelectric all-textile sensor arrays (TATSAs). By sewing these sensors into different sections of clothing, they achieved concurrent monitoring of arterial pulse waves and respiratory signals. This breakthrough lays the groundwork for innovations such as the electrically connected diode fiber proposed by Rein et al. [12], which was created through a scalable thermally drawn process. This fiber can serve as a fundamental building block for comprehensive fabric physiological monitoring systems in the future.

Apart from physiological parameters, the ability to monitor human daily motion is critical for joint health [13], rehabilitation, and chronic disease diagnosis. Mechanical sensors are instrumental in analyzing human motion, and smart fibers offer numerous promising outcomes. For example, Wang et al. [14] embedded magnetic fabric and conductive wires into clothing to generate a consistent and stable voltage and current when the wearer moves. In another innovation, Wang's team applied the principle of triboelectricity to develop self-powered motion-sensing capabilities. This innovation finds applications ranging from human motion [15] and gait monitoring to integration with artificial intelligence and motion-sensing systems [16].

Fiber and fabric-based electric sensors typically operate on principles of resistance or capacitance [17]. One of the key challenges in human motion monitoring is quantifying and spatially resolving deformations, which manifest as changes in these parameters. However, innovative solutions, such as the microstructure elastic fibers integrated with liquid metal conductors by Leber et al. [18], and Park et al. [19] fully textile-based highly stretchable structure, have been developed to address this issue. These solutions can precisely sense various human joint movements, including folding and rotation.

Beyond physiological and mechanical signals, wearable devices also need to account for environmental factors including humidity and temperature. Temperature/humidity-sensitive conductive composite fibers, created by incorporating conductive fillers into flexible insulating polymer matrices, exploit the linear or nonlinear resistivity changes of these materials with temperature or humidity [20]. Moreover, temperature/humidity sensing can be achieved by coating [21] or triggering chemical reactions [20] on the surface of fibers or yarns.

An essential feature of these smart fibers is their seamless integration into everyday life. They can be woven into fabrics or embedded into wearable devices, making health monitoring unobtrusive and comfortable. This ‘invisible’ integration does not disrupt the user’s routine, thus enhancing user adherence to health monitoring technologies. Moreover, these smart fabrics exhibit excellent biocompatibility, posing minimal risk of allergic reactions or skin irritation, making them suitable for continuous, long-term health monitoring. They are also durable and resistant to daily wear and tear, further promoting their use in everyday health monitoring systems [22].

The development of these novel fiber-based devices for health monitoring and protection represents a major stride toward more integrated, wearable, and user-friendly health monitoring technologies. The potential of these technologies to revolutionize the healthcare industry is immense, promising a future where preventative care and early diagnosis are the norms rather than the exceptions.

Significant research has been conducted on virtual sensor technology, yet our approach to virtualization distinguishes itself by its objectives. Unlike conventional applications, our virtualization strategy is designed to adapt to the ever-changing requirements of applications by fine-tuning system resource distribution and configuration settings. The typical applications of virtual sensors include.

- 1) *Fault Detection and Prevention*: Virtual sensors are instrumental in maintaining the system’s operational integrity. They analyze data patterns to identify anomalies or signs of performance decline early on, facilitating preemptive fault identification [23].
- 2) *Mitigation of Hardware Noise and Drift*: Environmental variations, equipment aging, and other factors can lead to noise and signal drift issues. Virtual sensors address these challenges through software algorithms, enhancing measurement precision [24].
- 3) *Enhanced Monitoring Capabilities*: By mitigating the necessity for costly or challenging-to-install physical sensors, virtual sensors prove invaluable, particularly in monitoring environments that are either hard to reach or extreme [25].

The virtualization of fabric hardware devices is a significant feature of big fiber slicing technology. Big fiber slicing achieves support for multiple types of applications under one hardware resource environment by focusing on the decoupling between hardware devices of fabric morphology and various practical applications. Through virtualization technology, it realizes the division of logical functions and parameter configuration collections according to the needs of specific services. It improves hardware resource utilization, enhances the efficiency of multiple tasks, and reduces latency.

In this section, we first introduce the virtualization scheme of fabric sensing units by controlling sampling rate, and sampling density, among others. We then analyze the settings of each layer unit, establish latency, data quality, and reliability models, and allocate virtual sensor and bandwidth resources for multiple applications. We have formulated an optimization problem that minimizes latency and maximizes data quality and reliability according to the different needs of each application.

III. SYSTEM ARCHITECTURE

This model calculates latency, data quality, and reliability score functions by constructing a physical sensing layer, a virtual sensing layer, and an Application layer, and establishing the corresponding dependencies between them. The optimal allocation strategy is found by solving to maximize the score function. The basic components and data flow of each layer are shown in Fig. 2:

- 1) *Physical Sensing Layer*: Multifunctional fibers utilize physical correlations, such as piezoelectric effects, and electromagnetic induction, to sense external stimuli and generate corresponding effect signals.
- 2) *Virtual Sensing Layer*: Each group of smart fabric sensing units is connected to a microprocessor. The microprocessor preliminarily processes the raw data and obtains the digital representation of physical characteristic variables in an invariant form, aggregated form, or other modified ways [25]. In this process, the precision, density, and range of sensing may all be enhanced. We optimize different virtual sensor nodes by controlling different sampling rates, sampling densities, anomaly processing, and data compression algorithms.
- 3) *Cloud-Native Application Layer*: Various types of cloud-based applications have different requirements for latency, data quality, and data reliability. By reorganizing the collection of virtual sensors, different slices are divided for cloud applications.

In this system, the problems to be solved are as follows: the allocation problem of virtual sensors and bandwidth resources. We hope to find the optimal allocation strategy for virtual sensors and bandwidth resources by analyzing the different applications’ needs for latency, data quality, and reliability.

A. Physical Sensing Layer

First, we categorize the hardware. According to the different physical quantities perceived by the fabric nodes, for example: pressure sensing fibers, and temperature sensing fibers, we represent groups of the same type of sensors as s_m , where m

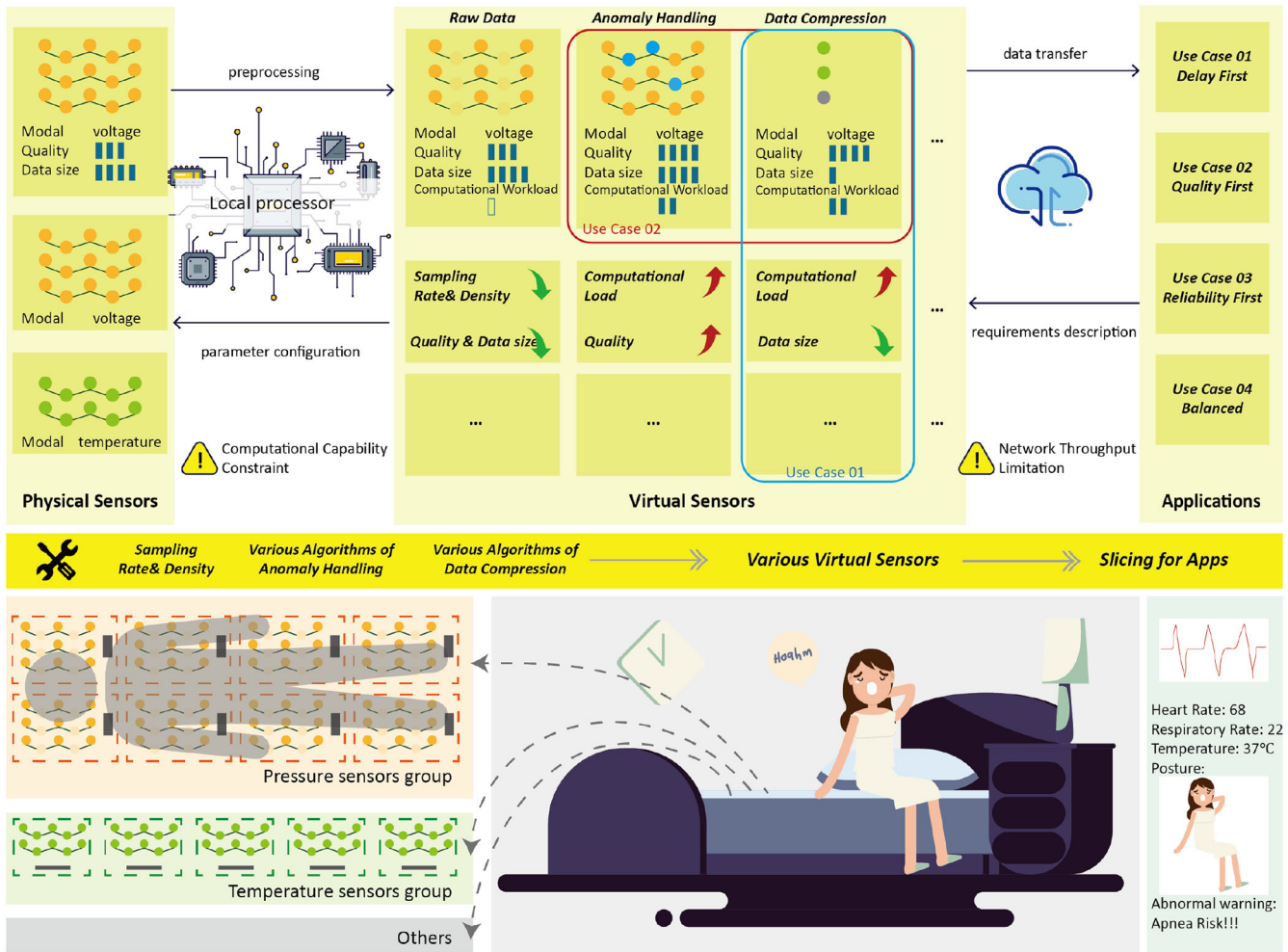


Fig. 2. System architecture of big fiber slicing.

denotes the type of sensors, $m \in \{1, \dots, M\}$, with a total of M groups of sensors.

Considering the different physical locations of the same type of fabric block, we can divide the fabric into B_m blocks, each connected to a microprocessor. $s_{m,i}$ represents the i th fabric block belonging to the m th type of sensor s_m , where $i \in \{1, \dots, B_m\}$. In this fabric block, there are a total of L_m sensor nodes.

B. Virtual Sensing Layer

To make full and better use of resources, we consider the allocation strategy of virtual sensors, rather than allocating the original hardware sensors directly.

To simplify the discussion, we only set up the following three virtualization schemes. For the i th block of the m th type of sensor, we classify the virtual sensors as follows.

- 1) $s_{m,i}^0$ represents the raw data directly extracted from the i th block of the sensor s_m .
- 2) $s_{m,i}^1$ represents the preprocessed data extracted from the i th block of the sensor s_m . The preprocessing operations include filling in missing values and handling outliers.
- 3) $s_{m,i}^2$ represents the data after data compression processing from the i th block of the sensor s_m . The main

consideration is lossless data compression methods, such as Huffman Encoding, Lempel-Ziv-Welch, etc.

C. Application Layer

At the upper layer of the fabric network, we consider N applications, denoted as A_n , where $n \in \{1, \dots, N\}$, each with different needs for latency, data quality, and reliability.

Application A_n has different requirements for latency, data quality, and reliability, and we assume that the weights for each requirement are $a_{n,del}$, $a_{n,qual}$, and $a_{n,rel}$, satisfying $a_{n,del} > 0$, $a_{n,qual} > 0$, and $a_{n,rel} > 0$, respectively.

Each application A_n has requirements for the types of sensors involved at the physical layer, denoted as \mathbb{M}_n , where $\mathbb{M}_n \subset \mathbb{M}$. Here, \mathbb{M} refers to the set of all types of sensors.

IV. ANALYSIS MODELS

To better enable applications to fully meet the requirements in terms of delay, data quality, and reliability, we should consider the different impacts of various virtual sensors on these requirement factors while allocating virtual sensors. Hence, we introduce Computational Load, Data Size, and Data Quality of the virtual sensors. We define a higher sampling rate and a higher sampling density as representing higher Data

TABLE I
LIST OF SYMBOLS

Symbol	Definition
A_n	Application n , where $n \in [1, N]$
B_m	Number of fabric blocks for sensor type m
L_m	Number of Sensor nodes in the fabric block for sensor type m
M	Number of sensor types
N	Number of upper-layer applications
\mathbb{M}	Set of all sensor types
\mathbb{M}_n	Set of sensor type demands for application A_n
$a_{n,\text{del}}$	Weight set by application n for delay
$a_{n,\text{qual}}$	Weight set by application n for quality
$a_{n,\text{rel}}$	Weight set by application n for reliability
s_m	Sensor of type m , where $m \in [1, M]$
$s_{m,i}$	Represents the i^{th} fabric unit of sensor type m
$s_{m,i}^k$	Represents the k^{th} virtual sensor for sensor unit $s_{m,i}$
$u_{n,m,i}^k$	Allocation status of the virtual sensor $s_{m,i}^k$ for application n , where $u_{n,m,i}^k \in \{0, 1, 2\}$
$r_{n,m,i}$	sampling rate of application n for the i^{th} block of sensor m
$d_{n,m,i}$	sampling density of application n for the i^{th} block of sensor m
r_m	The maximum sampling rate of sensor m
d_m	The maximum sampling density of sensor m
$C(\cdot)$	Function for calculating the computational cost for the corresponding sensor
$Q(\cdot)$	Function for calculating the data quality for the corresponding sensor
$S(\cdot)$	Function for calculating the total data for the corresponding sensor
$C_{\text{sum}}(A_n)$	The total computation for application n
$Q_{\text{sum}}(A_n)$	The total quality for application n
$Q_{\text{max}}(A_n)$	The maximum quality for application n
$S_{\text{sum}}(A_n)$	The total data amount for application n
$D_P(A_n)$	The computation delay for application n
$D_T(A_n)$	The transmission delay for application n
$D_{\text{sum}}(A_n)$	The total delay for application n
$R_{\text{sum}}(A_n)$	The total reliability for application n
$\text{Score}_{\text{del}}(A_n)$	Normalized delay score for application n
$\text{Score}_{\text{qual}}(A_n)$	Normalized quality score for application n
$\text{Score}_{\text{rel}}(A_n)$	Normalized reliability score for application n
$\text{Score}(A_n)$	Composite score for application n , including scores for delay, quality, and reliability
$\text{Score}_{\text{all}}$	Sum of the composite scores for all applications

Quality, while errors and corruption in the data itself will decrease Data Quality.

The Computational load, Data size, and Data Quality associated with virtual sensor $s_{m,i}^k$ can be represented as $C(m, k, r_{n,m,i}, d_{n,m,i})$, $S(m, k, r_{n,m,i}, d_{n,m,i})$, $Q(m, k, r_{n,m,i}, d_{n,m,i})$, where k refers to the virtual sensor number (as defined in the Table I).

Based on our Formulas for computational load, data size, data quality, and reliability, we can derive the scores in delay, data quality, and reliability for the allocation strategies of virtual sensors adopted for application A_n , and according to the different needs of application A_n , perform corresponding weighting to obtain a comprehensive score.

To calculate the corresponding score for application A_n , we first need to consider the allocation of virtual sensors for application A_n . For virtual sensors $s_{m,i}^0$, $s_{m,i}^1$, and $s_{m,i}^2$, we define the allocation index as

$$u_{n,m,i} \in \{0, 1, 2\}$$

where

$$n \in \{1, 2, \dots, N\}, m \in \mathbb{M}_n, \mathbb{M}_n \subset \mathbb{M}, i \in \{1, 2, \dots, B_m\}.$$

This represents which one in $s_{m,i}^0$, $s_{m,i}^1$ and $s_{m,i}^2$ application A_n uses. The sampling rate and sampling density of application n for the i^{th} block of sensor m are represented as $r_{n,m,i}$ and $d_{n,m,i}$, respectively.

We need to consider the following two constraints.

- 1) The computational power limitation of a single processor.
- 2) The overall network transmission bandwidth limitation. Additionally, there is a data buffer in the cloud, and parts exceeding the buffer are set to be discarded.

A. Latency Model

Before contemplating specific computation and transmission delays, we need to allocate the corresponding processing resources and transmission bandwidth to application A_n . Computational resources in microprocessors are specifically represented by the number of clock cycles.

According to our settings, each sensor block has a corresponding microprocessor. Considering the microprocessor i contained in sensor s_m , its computational resource is represented as $P_{m,i}$, and the processing resources provided to the slicing strategy are $P_{m,i}^0 > 0$, $P_{m,i}^1 > 0$, and $P_{m,i}^2 > 0$, and they satisfy

$$\sum_{j=0}^2 P_{m,i}^j \leq P_{m,i}. \quad (1)$$

Since the overall network bandwidth is limited, we need to allocate appropriate transmission bandwidth resources for each application A_n . Suppose that the total network bandwidth is T , and the transmission bandwidth resource provided to application A_n is $T_n > 0$, satisfying

$$\sum_{n=1}^N T_n \leq T. \quad (2)$$

To calculate the delay score for application A_n , we first need to compute the computation delay $D_P(A_n)$ and transmission delay $D_T(A_n)$ for application A_n

$$D_P(A_n) = \sum_{m \in \mathbb{M}_n} \sum_{i=1}^{B_m} \frac{C(m, j, r_{n,m,i}, d_{n,m,i})}{P_{m,i}^j} \Big|_{j=u_{n,m,i} \in \{0,1,2\}} \quad (3)$$

$$D_T(A_n) = \frac{\sum_{m \in \mathbb{M}_n} \sum_{i=1}^{B_m} S(m, j, r_{n,m,i}, d_{n,m,i}) \Big|_{j=u_{n,m,i} \in \{0,1,2\}}}{T_n}. \quad (4)$$

The formula above initially sums the total data of virtual sensors allocated to application A_n under each sensor type

and each block of that type. The transmission delay can then be obtained based on the transmission bandwidth resources allocated to application A_n .

Owing to the existence of cloud data buffers, parts exceeding the buffer will be discarded. Thus, the total delay $D_{\text{sum}}(A_n)$ for application A_n is considered to have an upper limit $D_{\text{max}}(A_n)$, i.e.,

$$D_{\text{sum}}(A_n) = \min(D_P(A_n) + D_T(A_n), D_{\text{max}}(A_n)). \quad (5)$$

B. Quality Model

We define the data quality of application A_n as

$$Q_{\text{sum}}(A_n) = \sum_{m \in \mathbb{M}_n} \sum_{i=1}^{B_m} Q(m, j, r_{n,m,i}, d_{n,m,i}) \Big|_{j=u_{n,m,i} \in \{0,1,2\}} \quad (6)$$

where $Q_{m,i}(\cdot)$ is a function related to the type of sensor and the corresponding sensor sampling rate and sampling density. We believe that a higher sampling rate and density result in higher data quality.

And we define the maximum data quality of application A_n as

$$Q_{\text{max}}(A_n) = \sum_{m \in \mathbb{M}_n} \sum_{i=1}^{B_m} Q(m, 2, r_{\text{max}}, d_{\text{max}}) \quad (7)$$

where $r_{\text{max}}, d_{\text{max}}$ is the maximum achievable sampling rate and density by application.

C. Reliability Model

Due to the cloud discarding data packets exceeding the data buffer's capacity, we cannot guarantee that all data will be received and processed. To measure this situation, we assess the reliability of application A_n . We believe that if an application can receive all the data completely, its reliability should be 1. Accordingly, we establish the reliability function for application A_n

$$R_{\text{sum}}(A_n) = \frac{D_{\text{sum}}(A_n) - D_P(A_n)}{D_T(A_n)}. \quad (8)$$

The above formula represents the ratio of the actual time used to send data to the theoretical time used to send data, i.e., the ratio of the actual data that should be sent to the theoretical data that should be sent, which is the reliability sought.

D. Score Model

To better evaluate latency, quality, and reliability, we define respective scoring functions. And to avoid the impact of numerical magnitude differences on requirement weights, we need to ensure that different scores are controlled within the range of 0 to 1 when calculating them.

As for the delay score should satisfy the requirement that the higher the delay, the lower the delay score. When delay is 0, the score is 1, and when delay reaches its upper limit, the delay score is 0. Additionally, delay is constrained by reliability. Hence, the delay score calculation formula, $\text{Score}_{\text{del}}$, is as follows:

$$\bar{\text{Score}}_{\text{del}}(A_n) = \frac{(D_{\text{max}}(A_n) - D_{\text{sum}}(A_n))}{D_{\text{max}}(A_n)} * R_{\text{sum}}(A_n). \quad (9)$$

For the data quality score, it satisfies that when application A_n achieves the maximum quality, the quality score is 1. The data quality score is also constrained by reliability. Hence, the quality score calculation formula, $\bar{\text{Score}}_{\text{qual}}$, is as follows:

$$\bar{\text{Score}}_{\text{qual}}(A_n) = \frac{Q_{\text{sum}}(A_n)}{Q_{\text{max}}(A_n)} * R_{\text{sum}}(A_n). \quad (10)$$

And the reliability score calculation formula, $\bar{\text{Score}}_{\text{rel}}$, is as follows:

$$\bar{\text{Score}}_{\text{rel}}(A_n) = R_{\text{sum}}(A_n). \quad (11)$$

E. Problem Formulation

The model designed in this article aims to derive an appropriate strategy for the allocation of virtual sensors and bandwidth resources, ensuring that the requirements for delay, data quality, and reliability of all applications are adequately met. In other words, it solves for the corresponding $u_{n,m,i}, r_{n,m,i}, d_{n,m,i}, T_n, P_{m,i}^j$ to maximize the overall score $\text{Score}_{\text{all}}$ of all applications, expressed as

$$\max_{u_{n,m,i}, r_{n,m,i}, d_{n,m,i}, T_n, P_{m,i}^j} \text{Score}_{\text{all}} = \sum_{n=1}^N \text{Score}(A_n). \quad (12)$$

Given the delay score, data quality score, and reliability score obtained from the above, and since application A_n has different demand weights for delay, data quality, and reliability, denoted as $a_{n,\text{del}} > 0$, $a_{n,\text{acc}} > 0$, and $a_{n,\text{rel}} > 0$, respectively, we can derive the overall score for application A_n as

$$\begin{aligned} \text{Score}(A_n) &= a_{n,\text{del}} * \bar{\text{Score}}_{\text{del}}(A_n) \\ &\quad + a_{n,\text{qual}} * \bar{\text{Score}}_{\text{qual}}(A_n) \\ &\quad + a_{n,\text{rel}} * \bar{\text{Score}}_{\text{rel}}(A_n). \end{aligned} \quad (13)$$

Ultimately, the problem can be expressed as

$$\begin{aligned} \max_{u_{n,m,i}, r_{n,m,i}, d_{n,m,i}, T_n, P_{m,i}^j} \text{Score}_{\text{all}} &= \sum_{n=1}^N (a_{n,\text{del}} * \bar{\text{Score}}_{\text{del}}(A_n) \\ &\quad + a_{n,\text{qual}} * \bar{\text{Score}}_{\text{qual}}(A_n) \\ &\quad + a_{n,\text{rel}} * \bar{\text{Score}}_{\text{rel}}(A_n)). \end{aligned} \quad (14)$$

Subject to

$$\begin{aligned} r_{n,m,i}, d_{n,m,i}, T_n, P_{m,i}^j &> 0, \text{ for all applicable } i, m, n \\ u_{n,m,i} &\in \{0, 1, 2\}, \text{ for all applicable } i, m, n \\ \sum_{n=1}^N T_n &\leq T \\ \sum_{j=0}^2 P_{m,i}^j &\leq P_{m,i} \text{ for all applicable } i, m \end{aligned}$$

where

$$\begin{aligned} n &\in \{1, 2, \dots, N\} \\ m &\in \mathbb{M}_n, \quad \mathbb{M}_n \subset \mathbb{M} \\ \mathbb{M} &= \{1, 2, \dots, M\} \\ i &\in \{1, 2, \dots, B_m\}. \end{aligned}$$

V. FS-MAPPO ALGORITHM

In this section, we utilize the MAPPO framework from reinforcement learning to solve our optimization problem, namely, by reasonably allocating virtual sensor resources and bandwidth resources, to realize the comprehensive maximization of delay, data quality, and reliability scores of each application.

A. Problem Transformation

To address the optimization problem, we first redefine our problem using the Markov Decision Process. The implementation of the algorithm relies on three elements closely related to the environment: state space, action space, and reward. Specifically, DRL allows the agent to observe the current state of the environment, select suitable actions for the environment to execute, and compute the corresponding returns to the agent. This process repeats so that the algorithm can obtain the maximum return from the environment after providing actions based on the current state. The state space, action space, and reward defined at time slot t are as follows.

- 1) *State Space*: To better design the state space and provide enough support for the generation of actions, based on our model construction, we design the computation delay $D_P^t(A_n)$, transmission delay $D_T^t(A_n)$, quality $Q_{\text{sum}}^t(A_n)$, and reliability $R_{\text{sum}}^t(A_n)$ involved in the application as the state space

$$s_t = \{D_P^t(A_1), D_T^t(A_1), Q_{\text{sum}}^t(A_1), R_{\text{sum}}^t(A_1), \dots, D_P^t(A_N), D_T^t(A_N), Q_{\text{sum}}^t(A_N), R_{\text{sum}}^t(A_N)\}. \quad (15)$$

- 2) *Action Space*: For the setting of the action space, we adopt a multidiscrete action space setup method. The action space includes five types of variables: the allocation of three corresponding virtual sensor types $u_{n,m,i} \in \{0, 1, 2\}$, the sampling rate $r_{n,m,i} \in \{1, 2, \dots, r_m\}$ and sampling density $d_{n,m,i} \in \{1, 2, \dots, d_m\}$, the allocation of microprocessor bandwidth resources $P_{m,i}^j \in \{1, 2, \dots, P_{m,i}\}$, and the allocation of transmission bandwidth resources $T_n \in \{1, 2, \dots, T\}$

$$a_t = \{u_{n,m,i}, r_{n,m,i}, d_{n,m,i}, P_{m,i}^j, T_n\}. \quad (16)$$

- 3) *Reward Space*: The reward is the composite score function obtained by weighted scores in delay, data quality, and reliability aspects determined by the current action and the state information generated by the action. This composite score can judge the quality of the action generated, and our goal is to maximize the composite score function $\text{Score}_{\text{all}} = \sum_{n=1}^N \text{Score}(A_n)$. During the learning process, the agent searches for the suitable allocation strategy to maximize the composite score, thus meeting the demands for delay, data quality, and reliability according to the needs of each application.

B. FS-MAPPO Algorithm

In this article, we employ the algorithmic architecture of MAPPO to solve our optimization problem and derive allocation strategies. As described in Algorithm 1, MAPPO

Algorithm 1 Optimization Algorithm using FS-MAPPO

Require: Application-related parameters, Sensor-related parameters, Number of iterations $Episode$, Maximum steps of training T_{max} .

- 1: Initialize θ , the parameters for policy π , and ϕ , the parameters for critic V , using Orthogonal initialization.
- 2: Initialize prioritized experience replay buffer R .
- 3: **for** episode = 1 to Episode **do**
- 4: Initialize environment to obtain the initial state s .
- 5: **for** $t = 1$ to T_{max} **do**
- 6: Select an action a based on state s .
- 7: Update $u_{n,m,i}, r_{n,m,i}, d_{n,m,i}, P_{m,i}^j, T_n$ and obtain the next state s' .
- 8: Obtain the reward $\text{Score}_{\text{all}} = \sum_{n=1}^N \text{Score}(A_n)$.
- 9: Store a new tuple (s, a, r, s') in the experience replay buffer R .
- 10: **if** R is sufficiently large **then**
- 11: Sample (s, a, r, s') through prioritized experience replay.
- 12: Update the actor by maximizing the function:

$$L(\theta) = \left[\frac{1}{Bn} \sum_{i=1}^B \sum_{k=1}^n \min \left(r_{\theta,i}^{(k)} A_i^{(k)}, \text{clip} \left(r_{\theta,i}^{(k)}, 1 - \epsilon, 1 + \epsilon \right) A_i^{(k)} \right) \right] + \sigma \frac{1}{Bn} \sum_{i=1}^B \sum_{k=1}^n S \left[\pi_{\theta}(o_i^{(k)}) \right] \quad (17)$$

- 13: Update the critic by minimizing the loss:

$$L(\phi) = \frac{1}{Bn} \sum_{i=1}^B \sum_{k=1}^n \max \left[\left(V_{\phi}(s_i^{(k)}) - \hat{R}_i \right)^2, \left(\text{clip} \left(V_{\phi}(s_i^{(k)}), V_{\phi_{\text{old}}}(s_i^{(k)}) - \epsilon, V_{\phi_{\text{old}}}(s_i^{(k)}) + \epsilon \right) - \hat{R}_i \right)^2 \right] \quad (18)$$

- 14: **end if**
- 15: **end for**
- 16: **end for**

trains two independent neural networks: an actor network with parameter θ and a value function network with parameter ϕ (known as the critic). Meanwhile, we enable these networks to be shared among all agents.

Specifically, the critic network, denoted as V_{ϕ} , performs the following mapping: $S \rightarrow \mathbb{R}$. The actor network, denoted as π_{θ} , maps the actor's observation $o_i^{(a)}$ to the categorical distribution of actions in the multidiscrete action space.

To train the actor network to maximize

$$s_t = \left\{ D_P^t(A_1), D_T^t(A_1), Q_{\text{sum}}^t(A_1), R_{\text{sum}}^t(A_1), \dots, D_P^t(A_N), D_T^t(A_N), Q_{\text{sum}}^t(A_N), R_{\text{sum}}^t(A_N) \right\} \quad (19)$$

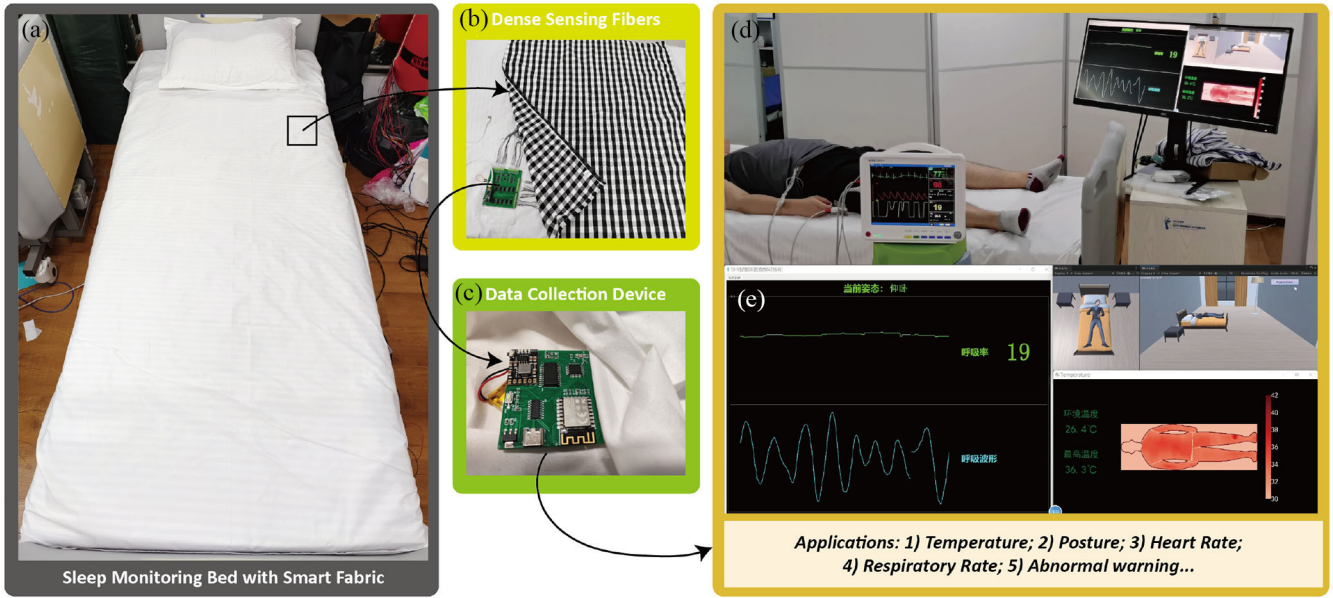


Fig. 3. Experimental platform of smart fabrics. (a) Sleep monitoring bed prepared with multifunctional fibers, including densely deployed pressure-sensing fibers, temperaturesensing fibers, and micro-motion-sensing fibers. (b) Schematic diagram of the connection between smart fabrics and data transmission equipment. (c) Data acquisition equipment, including acquisition modules, data processing modules, data transmission modules, and charging modules. (d) Experimental test results compared to medical devices. (e) Various application test result graphs, including heart rate, respiratory rate, temperature visualization, sleep position visualization, and abnormal warnings.

where

$$r_{\theta,i}^{(k)} = \frac{\pi_{\theta}(a_i^{(k)}|o_i^{(k)})}{\pi_{\theta_{old}}(a_i^{(k)}|o_i^{(k)})}. \quad (20)$$

$A_i^{(k)}$ is calculated using the GAE method, S is the policy entropy, and σ is the entropy coefficient hyperparameter.

To train the critic network, we minimize the loss function

$$L(\varphi) = \frac{1}{Bn} \sum_{i=1}^B \sum_{k=1}^n \max \left[\left(V_{\varphi}(s_i^{(k)}) - \hat{R}_i \right)^2, \left(\text{clip} \left(V_{\varphi}(s_i^{(k)}), V_{\varphi_{old}}(s_i^{(k)}) - \varepsilon, V_{\varphi_{old}}(s_i^{(k)}) + \varepsilon \right) - \hat{R}_i \right)^2 \right] \quad (21)$$

where \hat{R}_i is the discounted reward.

In the aforementioned loss functions, B represents the batch size, and n represents the number of agents.

VI. TESTBED AND PERFORMANCE EVALUATION

In this section, we evaluate the proposed FS-HAPPO scheme in conjunction with the smart fabric system we have constructed, as shown in Fig 3. We establish parameter schemes and validate system performance based on the semi-physical simulation platform we have built.

A. Experimental Setting

The fabric space is composed of three types of sensing fibers: Temperature Sensing Fiber (modal 0), Conventional Pressure Sensing Fiber (modal 1), and Micro-motion Pressure Sensing Fiber (modal 2).

We developed a universal data acquisition module (serving as an edge processor) that connects 16 channels of multifunctional fibers to a collection device. This system calculates the current physical quantity sensed through variations in voltage. The IC module is an ATMEGA328P-AU, featuring an Atmel AVR microprocessor with a system clock cycle of 20 MHz. The sampling system operates on the Arduino platform, storing each piece of data in 8 Bytes at a sampling rate of 32 Hz, which results in a total data volume of 4 kB per second for 16 channels. The communication module, model ESP-12F, transmits data over a Wi-Fi 4 (802.11n) network using the UDP protocol, with each UDP data packet capped at 1 kB.

In the virtualization layer, we established three types of virtualization schemes. Virtual Sensor 0 is set to acquire raw data without processing, where the sampling rate and density are adjustable, with a maximum of 32 Hz * 100%. Virtual Sensor 1 is configured for anomaly handling, using sliding filtering and mean filling. Experimental validation showed that each sample data requires at least 11 clock cycles. Virtual Sensor 2 is set for data compression, employing a lossless entropy compression algorithm. As indicated in literature [26], [27], this algorithm achieves a compression rate of approximately 70%, requiring about 12 instructions per saved bit. For simplicity, this analysis considers only the clock cycles needed for specific tasks, excluding other necessary operations.

In the application layer, four types of use cases are established, with weights for each indicator as shown in Table II.

B. Experiment 1: The Impact of Bandwidth Changes in Single Use Case Scenarios With Multimodal Data

We set the scenario as multidimensional information sensing and evaluation tasks in a fabric environment. Utilizing all three

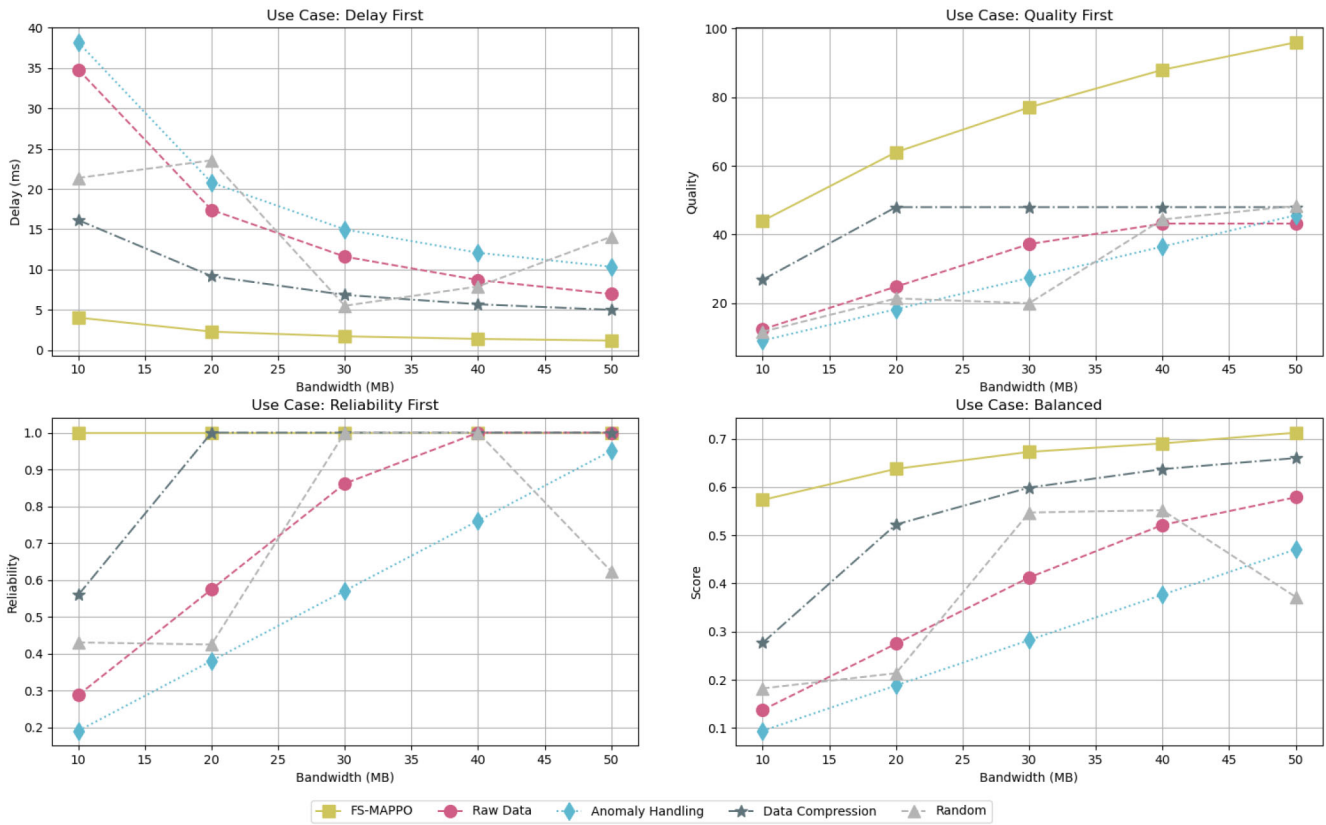


Fig. 4. Impact of bandwidth changes on indicators in one use case with multimodal data.

TABLE II
METRIC PREFERENCES FOR EACH USE CASE

	Latency	Quality	Reliability
Delay first	0.8	0.1	0.1
Quality first	0.1	0.8	0.1
Reliability first	0.1	0.1	0.8
Balanced	0.34	0.33	0.33

TABLE III
DATA MODALITIES AND PREFERENCE ACROSS EACH APPLICATION

	Modality	Preference
App 01	Temperature	Delay-first
App 02	Conventional pressure	Delay-first
App 03	Micro-motion pressure	Quality-first
App 04	Conventional & Micro-motion pressure	Quality-first
App 05	All 3 modalities	Balanced

types of sensor data, we compared the effects of bandwidth changes on latency, data quality, and reliability under different preference settings.

As shown in Fig. 4, our algorithm outperforms others in all preference settings, whether using raw data, performing anomaly handling, or data compression. Additionally, performing data compression in the microprocessor is a superior choice, as anomaly handling is limited by the microprocessor’s computational power.

C. Experiment 2: Incremental Application Changes Leading to Dynamic Resource Allocation

The experimental scenario was designed to reflect a dynamic system environment, where new application service requests continuously entered the system in the order of their application numbers. Specifically, at the first moment, only the needs of Application 1 were present, followed by the influx of Application 2’s requirements at the second moment, while retaining those of Application 1.

According to Fig. 5, it is evident that with the increase in applications, the performance of individual applications

declined slightly, characterized by a minor increase in latency, a slight decrease in reliability, and a reduction in data quality for certain applications. Overall, Applications 1 and 2, categorized as delay-first applications, exhibited very low overall latency but compromised data quality. In contrast, Applications 3 and 4, classified as quality-first applications, scored high in data quality, indicative of a greater volume of effective data, albeit with a corresponding increase in latency. Application 5, designed with a balanced preference, showed moderate performance across all metrics, as shown in Table III.

Fig. 6 presents a multidimensional evaluation of all five applications at the fifth moment in Fig. 5, when all applications were concurrently active. For Applications 1 and 2, which prioritized latency, our algorithm demonstrated superior performance in terms of overall system latency. For Applications 3 and 4, which emphasized data quality, our algorithm achieved the highest data quality. For Application 5, which had a balanced preference and utilized all three data modalities, our algorithm achieved the lowest latency and

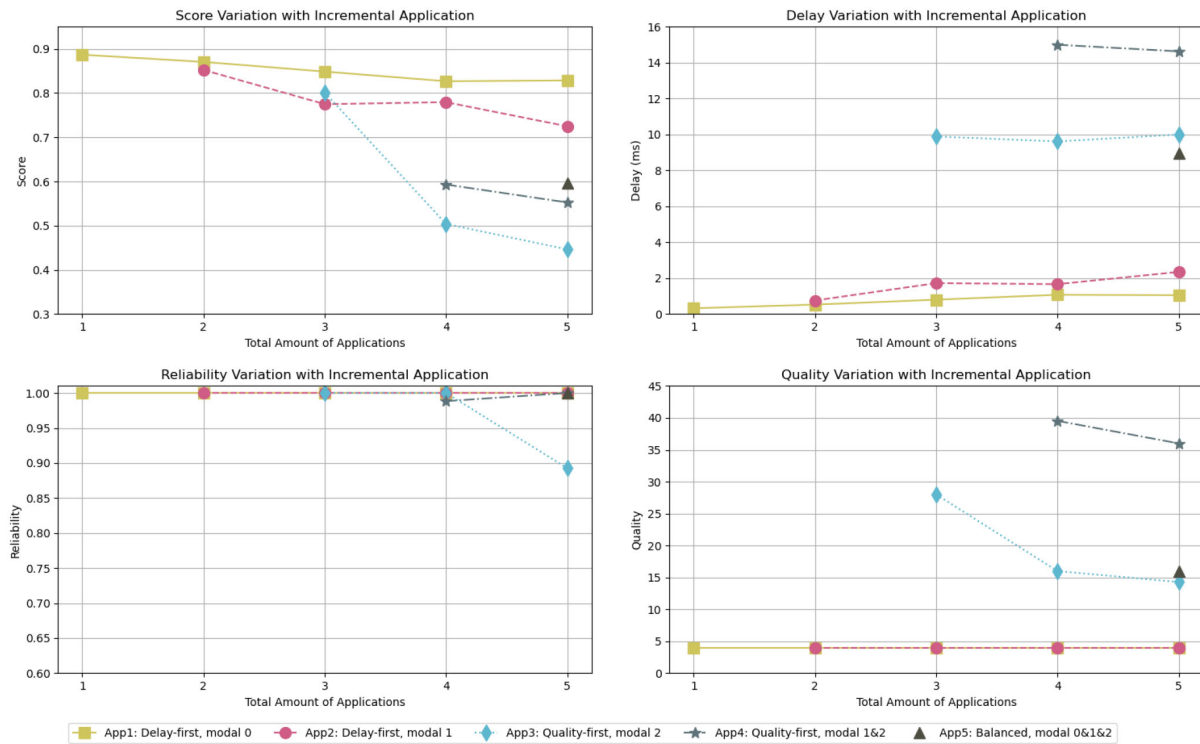


Fig. 5. Incremental application changes leading to dynamic resource allocation.

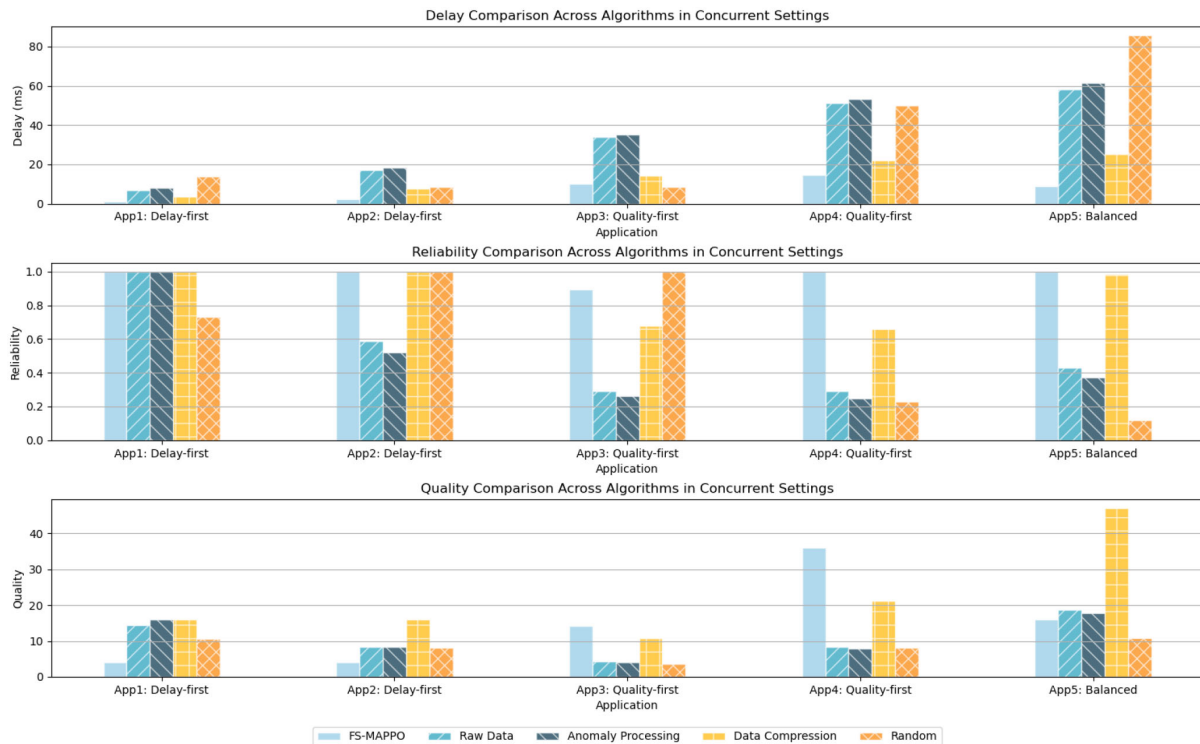


Fig. 6. Concurrent multiapplication performance: Algorithmic comparison.

highest reliability, though its data quality was not as high as methods using data compression.

In summary, our experimental results closely matched our initial expectations and hypotheses, demonstrating the effectiveness of our proposed allocation strategy across

various scenarios, whether for single or multiple applications with diverse needs. This finding carries substantial practical implications, especially in real-world deployments where computing and storage resources are limited, and applications often have unique demands regarding latency, quality, and reliability.

Traditional allocation methods struggle to optimize resource use while catering to the multifaceted requirements of different applications. Furthermore, the dynamic nature of application landscapes, characterized by frequent changes in quantity or type, underscores the importance of maintaining system robustness. Without adaptive adjustments, system performance can significantly deteriorate with changes. Our allocation strategy addresses this challenge by dynamically adapting parameter settings and resource distributions in response to application changes, thus ensuring optimized performance under various conditions.

VII. CHALLENGES FACED BY BIG FIBER TECHNOLOGY

As we push the boundaries of what is possible with smart fabrics, we inevitably encounter challenges that require careful consideration. While these fibers hold great promise as unobtrusive and real-time health monitoring, four notable issues stand in our way: fabric usability, data acquisition accuracy and stability, hardware circuit integration, and algorithm result reliability.

Fabric usability is crucial for ensuring the comfort, washability, and durability of smart fabrics. Striking the right balance of hardness, flexibility, stretch, air permeability, and skin affinity is essential to gain user acceptance. These fabrics should withstand multiple wash cycles while retaining their data acquisition functionalities, and they must maintain stable performance over extended use and time.

Data acquisition accuracy and stability are critical to preserving the accuracy and consistency of collected data in various environments and usage scenarios. Real-world situations present complex challenges, such as changes in fabric-skin adhesion due to human movement, variations in temperature and humidity caused by sweating, and optical effects from sunlight. Developing environmentally robust fabric sensors is essential to ensure reliable data acquisition.

Hardware integration involves the integration and encapsulation of the necessary hardware into the fabric for the health monitoring system. Current solutions often require printed circuit boards (PCBs) for signal acquisition, leading to large, hard PCBs and numerous wires that limit portability. To address this, future developments should focus on miniaturized, flexible, and highly integrated circuits.

Algorithm reliability is concerned with the accuracy and trustworthiness of the AI algorithms used for data analysis. The “black box” nature of deep learning necessitates rigorous and comprehensive validation, particularly in the medical field, to ensure the results are accurate and reliable.

Beyond these four challenges, other considerations arise in the broader application and future research of smart fabrics. These include managing the cost and quality of the fiber materials for large-scale clinical applications, ensuring the reusability and stability of the fibers, and addressing privacy and data security concerns associated with the data collected by the fibers.

The black box problem of AI algorithms also extends to the challenge of explainability. Due to systemic biases in clinical data collection, AI systems may suffer from a lack of representativeness, accuracy, and generalizability. Understanding

how these systems identify patterns and their implications on human-computer interaction can significantly impact the efficacy of AI in medical practice.

Each of these challenges presents both obstacles to overcome and opportunities for innovation. As we progress in the research and development of smart fabrics, this convergence of material science and computer science holds tremendous potential to revolutionize medical and health management, becoming significant player in advancing healthcare practices.

VIII. CONCLUSION AND FUTURE WORK

In this work, we propose a technology for virtualizing fabric sensors resources, named “Big Fiber Slicing,” to accommodate the dynamic and diversified requirements anticipated with the large-scale deployment of multimodal fiber devices in living environments. This technology entails the virtualization of multimodal physical sensors through various sampling, preprocessing, and data compression algorithms, followed by partitioning the virtual sensors into distinct “slices” tailored for specific use cases. The algorithm we developed is capable of automatically managing the allocation and scheduling of virtual resources based on application-specific demands, thereby optimizing resource utilization and enhancing user satisfaction. The separation of software from hardware afforded by virtualization technology facilitates the seamless upgrade and iteration of smart fabric systems, significantly improving their adaptability and scalability. Specifically, we first virtualize multimodal physical sensors according to different sampling, preprocessing and data compression algorithms, and then divide the virtual sensors into multiple independent “slices” for different use cases. Our algorithm can automatically realize the allocation and scheduling of virtual resources according to the different needs of the application, maximizing resource utilization and user satisfaction. Virtualization technology separates software and hardware, making it easier for smart fabric systems to be upgraded and iterated, and its adaptability and scalability are greatly improved.

The efficacy of our proposed solution was validated on an actual multimodal and multiapplication smart fabric platform. Our experiments demonstrated that the algorithm could meet the diverse preferences of various use cases, even under the constraints of limited network and edge processing capabilities. Furthermore, our slicing strategy was found to effectively manage optimal scheduling amid a continuous influx of varied application requests. Beyond the tested scenario of sleep monitoring, the “Big Fiber Slicing” technology holds potential for broader applications in edge intelligence scenarios, offering hardware resource scheduling solutions that can dynamically accommodate diverse application needs. For instance, in a smart home context, it enables the tailored allocation and scheduling of resources for wearable and environmental IoT devices, catering to the varied requirements of multiple household members across different times.

Looking ahead, the envisioning of intelligent health agents suggests a future filled with hope and transformative possibilities in life and health fields. These agents, equipped with capabilities ranging from vital signs monitoring to offering

surgical assistance and personalized post-operative therapies, promise to become unobtrusive yet integral components of our daily lives. However, realizing this future entails overcoming interdisciplinary challenges, and leveraging “Big Fiber Slicing” technology to blend the physical and intellectual aspects of medicine, material science, and AI. This approach not only paves the way for democratizing comprehensive health care but also signals a paradigm shift toward enhancing quality of life and longevity through intelligent health interventions.

REFERENCES

- [1] X. Li et al., “Network slicing for 5G: Challenges and opportunities,” *IEEE Internet Comput.*, vol. 21, no. 5, pp. 20–27, Sep. 2017.
- [2] X. Foukas, G. Patounas, A. Elmokashfi, and M. K. Marina, “Network slicing in 5G: Survey and challenges,” *IEEE Commun. Mag.*, vol. 55, no. 5, pp. 94–100, May 2017.
- [3] A. F. Abouraddy et al., “Towards multimaterial multifunctional fibres that see, hear, sense and communicate,” *Nat. Mater.*, vol. 6, no. 5, pp. 336–347, 2007.
- [4] L. Wang, Z. Lou, K. Jiang, and G. Shen, “Bio-multifunctional smart wearable sensors for medical devices,” *Adv. Intell. Syst.*, vol. 1, no. 5, 2019, Art. no. 1900040.
- [5] C. Li et al., “Design of biodegradable, implantable devices towards clinical translation,” *Nat. Rev. Mater.*, vol. 5, no. 1, pp. 61–81, 2020.
- [6] M. Chen, et al., “Multifunctional fiber-enabled intelligent health agents,” *Adv. Mater.*, vol. 34, no. 52, 2022, Art. no. 2200985.
- [7] H. Wang, Y. Zhang, X. Liang, and Y. Zhang, “Smart fibers and textiles for personal health management,” *ACS Nano*, vol. 15, no. 8, pp. 12497–12508, 2021.
- [8] Z. Li and Z. L. Wang, “Air/liquid-pressure and heartbeat-driven flexible fiber nanogenerators as a micro/nano-power source or diagnostic sensor,” *Adv. Mater.*, vol. 23, no. 1, pp. 84–89, 2011.
- [9] W. Fan et al., “Machine-knitted washable sensor array textile for precise epidermal physiological signal monitoring,” *Sci. Adv.*, vol. 6, no. 11, 2020, Art. no. eaay2840.
- [10] J. Song et al., “Mechanically and electronically robust transparent organohydrogel fibers,” *Adv. Mater.*, vol. 32, no. 8, 2020, Art. no. 1906994.
- [11] T. Li et al., “High-performance poly (vinylidene difluoride)/dopamine core/shell piezoelectric nanofiber and its application for biomedical sensors,” *Adv. Mater.*, vol. 33, no. 3, 2021, Art. no. 2006093.
- [12] M. Rein et al., “Diode fibres for fabric-based optical communications,” *Nature*, vol. 560, no. 7717, pp. 214–218, 2018.
- [13] H. Kainz, C. P. Carty, L. Modenese, R. N. Boyd, and D. G. Lloyd, “Estimation of the hip joint centre in human motion analysis: A systematic review,” *Clin. Biomech.*, vol. 30, no. 4, pp. 319–329, 2015.
- [14] R. Wang et al., “Magnetolectrical clothing generator for high-performance transduction from biomechanical energy to electricity,” *Adv. Funct. Mater.*, vol. 32, no. 6, 2022, Art. no. 2107682.
- [15] Z. Wen et al., “Self-powered textile for wearable electronics by hybridizing fiber-shaped nanogenerators, solar cells, and supercapacitors,” *Sci. Adv.*, vol. 2, no. 10, 2016, Art. no. e1600097.
- [16] J. Luo, W. Gao, and Z. L. Wang, “The triboelectric nanogenerator as an innovative technology toward intelligent sports,” *Adv. Mater.*, vol. 33, no. 17, 2021, Art. no. 2004178.
- [17] F. Salim, D. Prohasky, A. Belbasis, S. Houshyar, and F. K. Fuss, “Design and evaluation of smart wearable undergarment for monitoring physiological extremes in firefighting,” in *Proc. ACM Int. Symp. Wearable Comput. Adjun. Program*, 2014, pp. 249–254.
- [18] A. Leber, C. Dong, R. Chandran, T. D. Gupta, N. Bartolomei, and F. Sorin, “Soft and stretchable liquid metal transmission lines as distributed probes of multimodal deformations,” *Nat. Electron.*, vol. 3, no. 6, pp. 316–326, 2020.
- [19] S. Park et al., “Highly bendable and rotational textile structure with prestrained conductive sewing pattern for human joint monitoring,” *Adv. Funct. Mater.*, vol. 29, no. 10, 2019, Art. no. 1808369.
- [20] T. Q. Trung, H. S. Le, T. M. L. Dang, S. Ju, S. Y. Park, and N.-E. Lee, “Freestanding, fiber-based, wearable temperature sensor with tunable thermal index for healthcare monitoring,” *Adv. Healthcare Mater.*, vol. 7, no. 12, 2018, Art. no. 1800074.
- [21] J. Lee et al., “Intrinsically strain-insensitive, hyperelastic temperature-sensing fiber with compressed micro-wrinkles for integrated textronics,” *Adv. Mater. Technol.*, vol. 5, no. 5, 2020, Art. no. 2000073.
- [22] M. Chen, et al., “Imperceptible, designable, and scalable braided electronic cord,” *Nat. Commun.*, vol. 13, no. 1, p. 7097, 2022.
- [23] A. Bustillo, M. Correa, and A. Renones, “A virtual sensor for online fault detection of multitooth-tools,” *Sensors*, vol. 11, no. 3, pp. 2773–2795, 2011.
- [24] P. Albertos and G. C. Goodwin, “Virtual sensors for control applications,” *Annu. Rev. Control*, vol. 26, no. 1, pp. 101–112, 2002.
- [25] D. Martin, N. Kühl, and G. Satzger, “Virtual sensors,” *Bus. Inf. Syst. Eng.*, vol. 63, pp. 315–323, Jun. 2021.
- [26] K. L. Ketshabetswe, A. M. Zungeru, B. Mtengi, C. K. Lebekwe, and S. R. S. Prabaharan, “Data compression algorithms for wireless sensor networks: A review and comparison,” *IEEE Access*, vol. 9, pp. 136872–136891, 2021.
- [27] F. Marcelloni and M. Vecchio, “An efficient lossless compression algorithm for tiny nodes of monitoring wireless sensor networks,” *Comput. J.*, vol. 52, no. 8, pp. 969–987, Nov. 2009.



Jia Liu received the bachelor’s degree in computer science and technology from the University of Electronic Science and Technology of China, Chengdu, China, in 2020. She is currently pursuing the Ph.D. degree with the Embedded and Pervasive Computing Laboratory, School of Computer Science and Technology, Huazhong University of Science and Technology, Wuhan, China.

Her research interests include Internet of Things, fabric computing, and edge computing.



Huanke Zheng received the bachelor’s degree from the School of Mathematics, South China University of Technology, Guangzhou, China, in 2023, where he is currently pursuing the master’s degree with the Embedded and Pervasive Computing Laboratory, School of Computer Science and Engineering.

His research interests include machine learning, data analysis, and edge computing.



Dongkun Huo (Member, IEEE) received the B.S. degree in computer science and technology from the School of Computer and Information Engineering, Henan University, Kaifeng, China, in 2020, and the M.S. degree in computer technology from the School of Computer and Information Technology, Beijing Jiaotong University, Beijing, China, in 2022. He is currently pursuing the Ph.D. degree with the Embedded and Pervasive Computing Laboratory, School of Computer Science and Technology, Huazhong University of Science and Technology, Wuhan, China.

His research interests include MANET, edge computing, and digital twin.



Yixue Hao received the Ph.D. degree in computer science from Huazhong University of Science and Technology (HUST), Wuhan, China, in 2017.

He is an Associate Professor with the School of Computer Science and Technology, HUST. His current research interests include 5G network, Internet of Things, edge computing, edge caching, and cognitive computing.



Dusit Niyato (Fellow, IEEE) received the B.Eng. degree from King Mongkut's Institute of Technology Ladkrabang, Bangkok, Thailand, in 1999, and the Ph.D. degree in electrical and computer engineering from the University of Manitoba, Winnipeg, MB, Canada, in 2008.

He is a Professor with the School of Computer Science and Engineering, Nanyang Technological University, Singapore. His research interests are in the areas of sustainability, edge intelligence, decentralized machine learning, and incentive mechanism design.



Salman A. Alqahtani is currently a Full Professor with the Department of Computer Engineering, College of Computer and Information Sciences, King Saud University, Riyadh, Saudi Arabia. He also serves as a senior consultant in computer communications, integrated solutions, and digital forensics for few development companies, and government sectors in Saudi Arabia. His main research interests include radio resource management for wireless and cellular networks (4G and 5G), Internet of Things, Industry 4.0, and digital forensics.



Min Chen (Fellow, IEEE) has been a Full Professor with the School of Computer Science and Engineering, South China University of Technology, Guangzhou, China. He is also the Director of the Embedded and Pervasive Computing Laboratory, Huazhong University of Science and Technology (HUST), Wuhan, China. He was an Assistant Professor with the School of Computer Science and Engineering, Seoul National University, Seoul, South Korea, before he joined HUST.

Dr. Chen was selected as a Highly Cited Researcher from 2018 to 2022. He got the IEEE Communications Society Fred W. Ellersick Prize in 2017, the IEEE Jack Neubauer Memorial Award in 2019, and the IEEE ComSoc APB Outstanding Paper Award in 2022. He is the Chair of IEEE Globecom 2022 eHealth Symposium. His Google Scholar Citations reached 45 000+ with an H-index of 97. His top paper was cited 4500+ times. He is the Founding Chair of the IEEE Computer Society Special Technical Communities on Big Data.